Structural Factors of Rigid−Coil Polymer Pairs Influencing Their Self-Assembly in Common Solvent

Min Kuang, Hongwei Duan, Jing Wang, and Ming Jiang*

Department of Macromolecular Science and The Key Laboratory of Molecular Engineering of Polymers, Fudan University, Shanghai, 200433, China

Received: April 18, 2004; In Final Form: July 25, 2004

This study investigates factors in the structure of rigid and coil polymer pairs that influence their self-assembly in solution. Several pyridine-unit-containing polymers, that is, poly(4-vinyl pyridine) (P4VP), poly(2-vinyl pyridine) (P2VP), copolymers of styrene and 4-vinyl pyridine (SVP), and PS-b−P2VP block copolymer, were used. Their counterparts, the rigid proton-donating polymers, that is, carboxyl-ended polyimide (PI) and poly(amic acid) ester (PAE), were used. All such rigid−coil polymer pairs could self-assemble into hollow aggregates of submicrometer size in their common solvents. The results show a common trend that the hydrodynamic radius of the assembled hollow spheres decreases with the increasing ratio of the rigid proton-donating polymer to the flexible proton-accepting polymer. A new route of micellization of block copolymers with the aid of the rigid polymers is presented. Structure stabilization of hollow spheres composed of PAE/PS-b−P2VP was successfully realized. Furthermore, crosslinking different parts of the hollow spheres led to nanocages totally different in chemistry: crosslinking PAE led to PAE-based nanocages while crosslinking P2VP blocks led to block-copolymer-based nanocages with the rigid PAE chains inside.

Introduction

There is progressively increasing interest in polymeric self-assembled objects in solutions with sizes ranging from the nanometer to the micrometer scale because of their many potential applications as carriers of catalysts, enzymes, drugs, etc.[1] In this connection, micellization of block copolymers has been extensively studied.[2] In addition to the traditional way of obtaining micelles of block copolymers in selective solvents, in which the two component blocks possess a large difference in solubility, several new routes to the micelles have been proposed: by altering the temperature,[3] by changing the pH value,[4] by chemically modifying one of the blocks,[5] by introducing a polymer having electrostatic interaction[6] or hydrogen bonding[7] with one of the blocks, by complexation of one block with organic molecules having a polar head and a nonpolar tail in water, etc.[8] Quite recently, we found that mixing a block copolymer containing the poly(vinyl pyridine) block with formic acid led to micelles through complexation between the carboxyl and pyridine groups.[9] In all such new routes, the driving force for the micellization is, in the final analysis, differential solubility between the blocks, although in some cases it is achieved by environmental changes or the chemical reactions.

Among the variety of self-assembled nanostructures of block copolymers, the micelles with an inner cavity (e.g., hollow spheres) have attracted special attention because of their great potential in the encapsulation of large-size molecules or a large numbers of molecules. Wooley et al.[10] and Liu et al.[11] produced hollow spheres by self-assembly of block copolymers into core−shell micelles followed by crosslinking the shell and degrading the core. Diverse hollow spheres can also be prepared by the "layer-by-layer" (LBL) technique[1f,12] using alternate depositions of oppositely charged species on various templates, and subsequently sacrificing the cores. In addition, using vesicles and particles as templates in in situ polymerization to produce hollow spheres has been reported.[13] Rod−coil block copolymers were found to be able to form large-size hollow spheres directly in their selective solvent.[14] Recently, several new approaches to hollow spheres have appeared in the literature, namely, assembly of amphiphilic graft copolymers at the oil−water interface,[15] cooperative assembly of nanoparticles of silica and gold with block copolypeptides,[16] formation of core−shell particles based on polycondensation of organosilanes followed by removal of nonbonded chains from the core,[17] etc.

Our group has developed new approaches to polymeric micelles and hollow spheres via interpolymer complexation in solutions.[18] For example, noncovalently connected micelles (NCCM) with poly(4-vinylpyridine) (P4VP) as the shell and hydroxyl-containing polystyrene as the core were formed in a selective solvent mixture for P4VP by interpolymer hydrogen bonding. Then, crosslinking the shell and removing the core by simple dissolution led to hollow spheres.[18c] More recently, we found that mixing of flexible homopolymer P4VP and a *rodlike or rigid polymer*, polyimide with carboxyl ends in their *common solvents*, can directly produce hollow spheres with sizes in hundreds of nanometers.[18e] For the obtained assemblies, a double-layered structure consisting of an outer shell of coil polymers, for example, P4VP, and an inner shell of the rigid polymer was suggested (Figure 1). Furthermore, when a crosslinkable rigid polymer was used for the assembly, the resulting hollow spheres could be stabilized by a simple photo crosslinking reaction.[19] The driving force of this unexpected self-assembly of the rigid−coil polymer pair is believed to be a combination of the requirement of effective packing of the rigid polymers and the "graft" architecture nature of the obtained complex.[18e,19,20] Compared with the existing procedures for producing micelles and hollow spheres, this process seems much simpler and more straightforward.

* mjiang@fudan.edu.cn.

10.1021/jp048314m CCC: $27.50 © 2004 American Chemical Society
Published on Web 09/16/2004

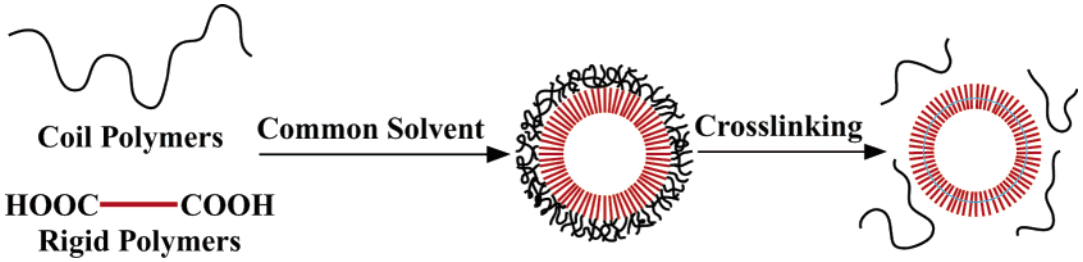

Figure 1. Schematic illustration of the formation of hollow spheres.

SCHEME 1: Chemical Structures of Poly(Amic Acid) Ester (PAE) and Polyimide (PI and PI-1)

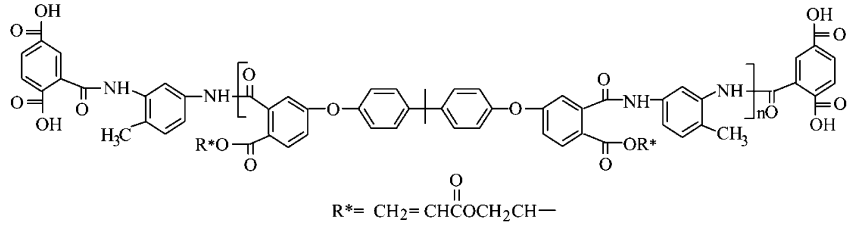

Poly(amic acid) Ester (PAE)

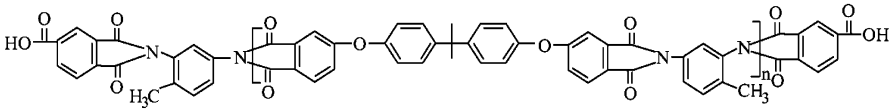

Polyimide (PI)

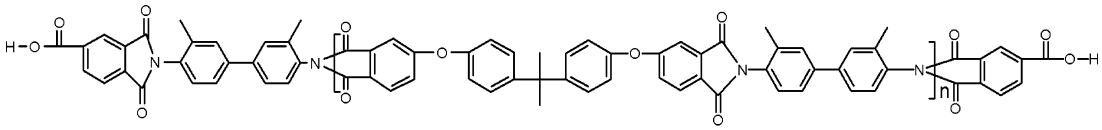

Polyimide-1 (PI-1)

This paper has two major aims. The first aim is to examine how the structural factors of the rigid and coil polymer components influence their self-assembly in their common solvent. For this, several pyridine-unit-containing polymers with different structures, that is, P4VP, poly(2-vinyl pyridine) (P2VP), as well as the copolymers of styrene and 4-vinyl pyridine (SVP), were used. For their counterparts, the rigid proton-donating polymers, we used carboxyl-ended polyimide (PI, Scheme 1) and poly(amic acid) ester (PAE, Scheme 1). The second aim is to seek new routes of micellization of block copolymers with the aid of rigid polymers. This possibility has been explored specifically using block copolymer of PS-b−P2VP. In both cases, much effort was devoted to make the assembled hollow spheres stable by photo and chemical crosslinking.

Experimental Section

Sample Preparation. The PI (Scheme 1) with two carboxyl ends was synthesized by condensation polymerization of bisphenol A dianhydride and 2, 4-diaminotoluence and then capped with trimellitic anhydride in dimethylacetamide at room temperature. This was followed by chemical imidization with acetic anhydride and triethylamine and thermoimidization up to 200 °C. The molecular weights were determined by size exclusion chromatography using THF as the eluent based on polystyrene calibration. Its number-average molecular weight is 9250 g/mol. By introducing photosensitive vinyl structure into PI prepolymer, PAE (Scheme 1) with two carboxyl ends was synthesized.[19] The number-average molecular weight of PAE is 7450 g/mol. The PS-b−P2VP block copolymer was synthesized and characterized as described by Zhao et al.[21] The M_w and PDI of the sample are 1.2×10^4 g/mol and 1.30, respectively, and the molar ratio of P2VP and PS blocks based on NMR analysis is about 1.5. The P4VP and P2VP were synthesized by free radical polymerization and the average molecular weights, M_η, are 1.4×10^5 g/mol and 2.0×10^5 g/mol. Accordingly, the numbers of the repeating unit are 1330 and 1900, respectively. The copolymers SVP32, SVP16, and SVP11 (the numerals denote the molar fraction of 4-vinyl pyridine) were synthesized by free radical copolymerization of styrene and 4-vinyl pyridine. The respective molecular weights (kg/mol) were 51.9, 29.4, and 26.7, and they were determined by size exclusion chromatography using DMF as the eluent based on polystyrene calibration.[20]

Preparation of Hollow Aggregates. A desired amount of PI (PAE) dilute solution in chloroform (or PAE in THF) was added dropwise to P4VP (or P2VP, PS-b−P2VP) solution in chloroform (THF, in the case of PAE) under ultrasonic conditions. In the final solution the concentration of P4VP (or P2VP, PS-b−P2VP) was 1.0×10^{-4} g/mL and the concentration of PI (or PAE) depended on the required ratio of PI (PAE)/P4VP (or P2VP, PS-b−P2VP). With the addition of PI (or PAE) solution, the solution turned slightly bluish, which indicated the formation of aggregates of PI/P4VP (or P2VP, PS-b−P2VP).

Structure Stabilization. The crosslinking of PAE is performed by irradiation of the aggregate solutions in THF under a high-pressure mercury lamp (365 nm, 300 W). To obtain the

PS-b−P2VP copolymer crosslinked hollow spheres, 100 mol % of 1,4-dibromobutane based on the pyridine units in the hollow spheres of PAE and PS-b−P2VP was added and the mixture was kept at 45 °C for 2 days.

Dynamic Light Scattering (DLS). A commercial laser light scattering (LLS) spectrometer (Malvern Autosizer 4700) equipped with a multi-τ digital time correlation (Malvern PCS7132) and a solid-state laser (ILT 5500QSL, output power = 100 mW at λ_0 = 514.5 nm) as the light source was used. The line-width distribution $G(\Gamma)$ can be calculated from the Laplace inversion of the intensity time correlation function into a transitional diffusion coefficient distribution $G^{(2)}(q, t)$. The inversion was carried out by the CONTIN program supplied with the Malvern PCS7132 digital time correlator. Using the Stokes−Einstein equation, $R_h = k_B T/6\pi\eta D$, where, k_B, T, and η are the Boltzmann constant, the absolute temperature, and the solvent viscosity, respectively, $G(\Gamma)$ can be converted into a transitional diffusion coefficient distribution $G(D)$ or a hydrodynamic radius distribution $f(R_h)$. Dust-free procedure was performed for the component solutions before mixing. All the measurements were done at 25.0 ± 0.1 °C.

Transmission Electron Microscopy. The TEM observations were performed on a Philips CM120 electron microscope at an accelerating voltage of 80 kV. In the preparation of the specimen for observing the discrete aggregates, 5 μL of the aggregate solution was dropped onto a carbon-coated copper grid, which was frozen in liquid N_2 just before being used. This was followed by solvent evaporation at room temperature.

Scanning Electron Microscopy. The SEM observations were performed on a Philips XL30 electron microscope at an accelerating voltage of 20 or 25 kV. For the sample preparation, a carbon-coated grid was dipped quickly into the micellar solution and then was dried in a flow hood at room temperature. The specimens were coated with gold before SEM observations.

Atomic Force Microscopy. The AFM imaging was performed with the aid of a Nanoscope III-M system operating in tapping mode. Samples for AFM imaging were prepared by placing a 2-μL drop of micellar solution on freshly cleaved mica and allowing it to dry freely at room temperature.

Results and Discussion

Self-Assembly of PI and P4VP (P2VP) into Hollow Spheres. In our previous communication,[18e] we reported that mixing PI-1 (Scheme 1) and P4VP in their common solvent $CHCl_3$ led to submicron-size hollow spheres with PI-1 as the inner shell and P4VP as the outer shell. We also recently found that self-assembly of a crosslinkable rigid polymer (e.g., photosensitive PAE and P4VP in THF) also led to hollow aggregates with an outer P4VP shell and an inner PAE shell.[19] The key factors affecting the self-assembly of these two polymer pairs are believed to be the hydrogen bonding between the carboxyl end groups of PI-1 (or PAE) and pyridine units of P4VP and the requirement of parallel packing of the "grafted" rigid PI-1 (or PAE) rods. In this study, a polyimide (PI) with a structure different from, and possibly more rigid than PI-1 was used. Herein, we studied this self-assembly of PI and P4VP in chloroform over a composition of PI/P4VP (w:w) ranging from 10.0 to 5.0. Accordingly, the chain number ratio of PI to P4VP was between 512 and 256. The dynamic light scattering results (Figure 2) for the blend solutions of PI/P4VP clearly demonstrate the formation of the submicron-size aggregates. It is interesting to see that although both P4VP and PI are polydispersed homopolymers and there are no chemical bonds between them, the aggregates display narrow size distributions as indicated by the small polydispersity index (PDI). As an example, the PI/P4VP (10:1, w:w) aggregates with numerous folds in SEM observation (Figure 3) clearly show their hollow nature.[12a] Combining the previous results using polyimide PI-1 and the present ones, we conclude that the chemical structure of the rigid polymer as a building block has little effect on their self-assembly and that this assembly of rigid−coil polymer pairs into hollow spheres is a general phenomenon.

When the coillike polymer P4VP was replaced by P2VP, micelles could also be obtained. The broken particles in the SEM image (Figure 4) again prove the hollow structure of the aggregates. Table 1 shows the hydrodynamic radius of PI/P2VP as a function of the blend composition. Two systems of PI/P4VP and PI/P2VP show the same variation trend. That is, over

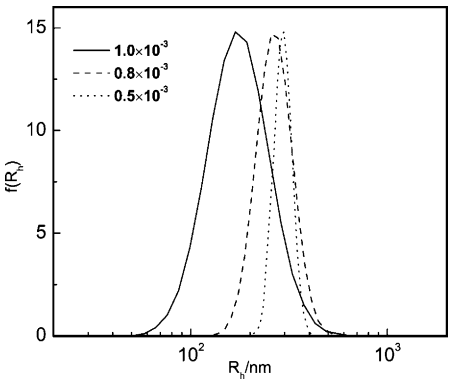

Figure 2. Hydrodynamic radius distribution of the PI/P4VP hollow particles in $CHCl_3$ with different composition. In the final solution, $C_{P4VP} = 1.0 \times 10^{-4}$ g/mL; C_{PI} is shown in the legend.

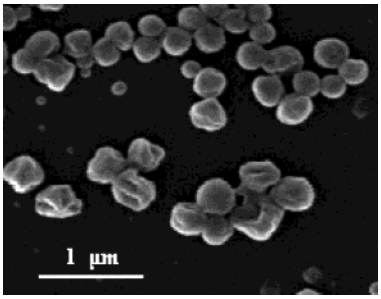

Figure 3. SEM images of hollow aggregates with PI/P4VP weight ratio of 10:1.

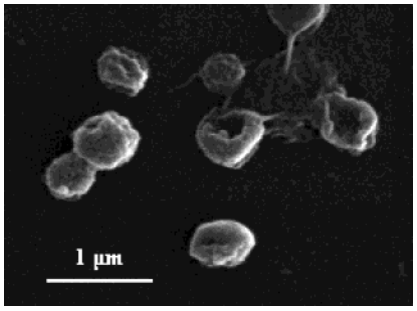

Figure 4. SEM images of hollow aggregates with PI/P2VP weight ratio of 10:1.

TABLE 1: Characterization Data of the Hollow Spheres of PI/P4VP(P2VP) Measured by Dynamic Light Scattering

	PI/P4VP		PI/P2VP	
C_{PI} 10^3 g·mL^{-1}	$\langle R_h \rangle$, nm	PDI	$\langle R_h \rangle$, nm	PDI
1.0	174	0.13	201	0.09
0.8	265	0.04	295	0.07
0.5	297	0.01	320	0.12

TABLE 2: Characterization Data of the Hollow Spheres of PAE/P4VP (P2VP, SVP*n*) Measured by Dynamic Light Scattering

	PAE/P4VP		PAE/P4VP (crosslinked)		PAE/P2VP		PAE/SVP32	
C_{PAE} 10^3 g·mL^{-1}	$\langle R_h \rangle$, nm	PDI	$\langle R_h \rangle$, nm	PDI	$\langle R_h \rangle$, nm	PDI	$\langle R_h \rangle$, nm	PDI
1.0	98	0.04	83	0.09	89	0.05	265	0.12
0.8	115	0.07	90	0.02	117	0.04	315	0.15
0.5	121	0.05	105	0.03	147	0.01	352	0.18

the composition range, $\langle R_h \rangle$ apparently increases with a decrease in the ratio of PI/P4VP (P2VP) from 10.0 to 5.0. This means that more grafts favor the formation of small aggregates. As discussed in our previous papers, it is the propensity to parallel packing of the PI grafts that results in the hollow spheres. Obviously, the larger the value of PI/PVP, the larger the "grafted density" of PI along the PVP chains. Consequently, such dense grafts promote the fine dispersion. This trend of the aggregate size varying with the "graft density" is similar to that reported for the micelles of graft copolymers[22] and hydrogen-bonding "graft copolymers"[18b] in selective solvents, although the mechanism for the aggregate formation is different. Comparing the two groups of data in Table 1, it is clear that at the same composition the micelles of PI/P4VP are always smaller than those of PI/P2VP. This can be attributed to the fact that P4VP obviously possesses less steric hindrance for its complexation with PI than P2VP does. Therefore, P4VP can connect with more PI grafts and thus obviously favors the formation of small aggregates.

Formation and Structural Fixation of Hollow Spheres Composed of PAE and Pyridine-Containing Polymers. We designed and synthesized PAE having a similar structure with PI but carrying two vinyl groups in each repeat unit and *double* carboxyl groups at both ends. Using PAE helps us to learn more about the end-group effect. It also particularly provides the possibility to attain structure-fixed hollow spheres by subsequent crosslinking of PAE in the resulting aggregates. It was found that by mixing the PAE and P4VP in their common solvent, THF, hollow aggregates could also formed.[19] The DLS data in Table 2 show that the aggregates have an average radius of around 100 nm with a narrow distribution, as indicated by the low PDI. Meanwhile, the size of the aggregates increases as the weight ratio PAE/P4VP decreases. Just as PI does, PAE can also self-assemble with P2VP. Figure 5 shows that $\langle R_h \rangle$ of the aggregates at a PAE/P2VP weight ratio of 10.0 is 89 nm, and it slightly increases with a decrease in the weight ratio from 10.0 to 5.0. A remarkable difference in size between PAE/P4VP (P2VP) and PI/P4VP (P2VP) can be found: at the same weight ratio, the $\langle R_h \rangle$ of the former is much smaller than that of the latter. As the molecular weights of PAE and PI are in the same order, the structural difference in the end groups (i.e., double-carboxyl ends in PAE and mono-carboxyl ends in PI (Scheme 1)), in our opinion, is responsible for the large difference. Obviously, the double ends in PAE favor the complexation leading to more grafts for each main chain and, consequently, smaller aggregates. In fact, in our previous studies on the interactions of coil-coil polymer pair, that is, carboxyl-end polystyrene and P4VP in chloroform, we found that the hydrogen-bonding grafting of PS with *double*-carboxyl ends to P4VP was much stronger than *mono*-carboxyl-ended PS.[23]

As another way of changing the "graft" density of PAE, we tried to use copolymer of SVP32, in which the interaction sites (pyridine) and inert polystyrene units were randomly distributed, to replace P4VP (P2VP). The DLS data in Table 2 for PAE/SVP32 reveal that supramolecular aggregates could also be obtained with a much larger size and a much broader distribution than those of PAE/P4VP (P2VP).The PAE/SVP32 also shows an apparent dependence of the aggregation on the composition, that is, the size decreases with the increasing ratio of PAE/SVP32. For SVP16 and SVP11, no aggregates with PAE in the solutions were detected by DLS. However, it was found that they were able to form aggregates with PAE in a selective solvent THF/cyclohexane (2:8, v:v), which could dissolve SVP but not PAE. In short, there is a minimum value of the relative amount of the proton-accepting groups along the chain for forming hollow spheres.

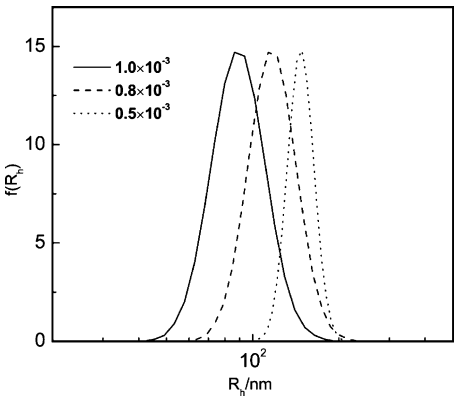

Figure 5. Hydrodynamic radius distribution of the PAE/P2VP hollow spheres in THF with different composition. In final solution, $C_{P2VP} = 1.0 \times 10^{-4}$ g/mL; C_{PAE} is shown in the legend.

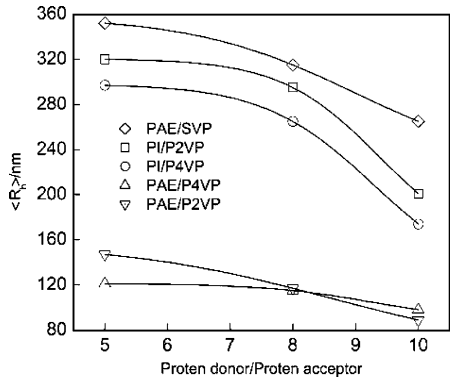

Figure 6. The $\langle R_h \rangle$ of hollow aggregates formed from different types of proton donor and proton acceptor pairs vs. the weight ratio of the proton-donating polymer to proton-accepting polymer, $C_{acceptor} = 1.0 \times 10^{-4}$ g/mL.

All the results mentioned above are summarized in Figure 6. Although there is a distinct structural change among these proton-donating polymers, as well as in the proton-accepting polymers, all the rigid−coil polymer pairs could self-assemble into aggregates in a submicrometer size. In addition, all the five polymer pairs studied show a common trend: the hydrodynamic radius of the assembled hollow spheres decreases with increases in the ratio of the rigid proton-donating polymer to the flexible proton-accepting polymer. Besides, it is clear that when PAE is used the aggregates have much finer dispersion, as their average size is less than half of the corresponding hollow spheres with PI as the proton-donating polymer. It clearly proves that the effect of the double end groups in PAE is remarkable as the groups evidently improve the interaction ability with the proton-accepting polymers compared to the single carboxyl-end polymers.

In the aggregates the inner shell and outer shell are connected by hydrogen bonding rather than chemical bonding, therefore

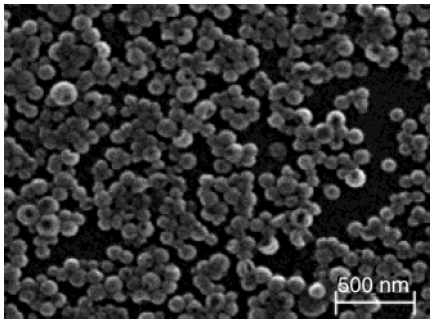

Figure 7. The SEM image of crosslinked PAE hollow spheres in DMF; in its precursor the PAE/P4VP weight ratio was 10:1.

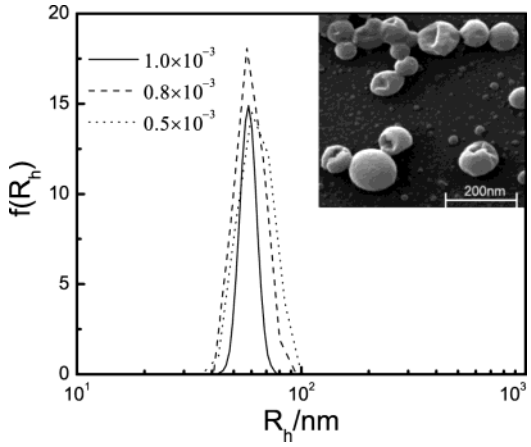

Figure 8. Hydrodynamic radius distribution of the PAE/PS-b−P2VP hollow particles in THF with different composition. In final solution, $C_{PS-b-P2VP} = 1.0 \times 10^{-4}$ g/mL; C_{PAE} is shown in the legend. The inset is the SEM observation of hollow spheres with a PAE/PS-b−P2VP weight ratio of 10:1.

the structures are sensitive to their environmental changes. To address this challenge, the hollow spheres with a stabilized structure were realized by crosslinking PAE under UV irradiation. After 5 min of irradiation at room temperature, an equivolume of DMF, which could cause dissociation of the interpolymer hydrogen bonding, was added into the solution. For a control solution without irradiation, adding DMF caused dissociation of the aggregates as monitored by DLS. In the case of PAE/P4VP, DLS (Table 2) showed that the crosslinked particles kept their monomodal distribution, which meant that there was no interparticle crosslinking. After adding DMF, the sizes of the aggregates decline by tens of nanometers as a result of removal of the outer shell P4VP due to dissociation of hydrogen bonding. Observation by SEM clearly shows monodispersed hollow spheres (Figure 7), which means that their structure was successfully locked in by crosslinking.

Self-Assembly of Block Copolymer PS-b−P2VP and PAE (PI). As discussed in the Introduction, in recently years, many new approaches to micelles of block copolymers have been proposed. However, the basic driving force for the assembly is still the solubility difference between the component blocks. With the aid of our experience in the assembly of rigid−coil polymer pairs, we have been thinking of a new mechanism of micellization of block copolymers in the presence of rigid chains.

Mixing the PS-b−P2VP and PAE solutions in their common solvent THF led to a bluish tinge. This indicated the formation of nanosize or microsize particles. Figure 8 shows the hydrodynamic radius distribution of the aggregates. Nanoparticles with a radius of about 60 nm were formed; their size distributions

TABLE 3: Characterization Data of the Hollow Spheres of PAE/PS-b−P2VP Measured by Dynamic Light Scattering

		before crosslink		PAE (crosslinked)		P2VP (crosslinked)	
sample	$C_{PAE}\ 10^3$ g·mL^{-1}	$\langle R_h \rangle$, nm	PDI	$\langle R_h \rangle$, nm	PDI	$\langle R_h \rangle$, nm	PDI
PAE-block	1.0	58	0.01	54	0.09	72	0.27
PAE-block	0.8	62	0.08	58	0.02	74	0.26
PAE-block	0.5	66	0.09	63	0.08	79	0.23

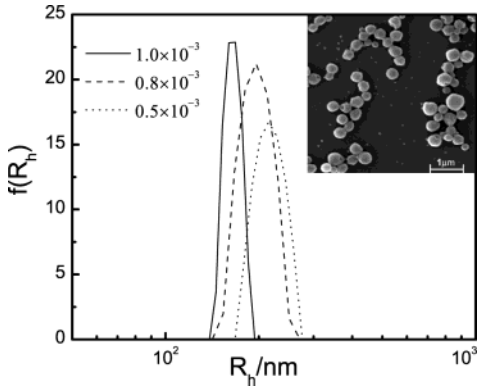

Figure 9. Hydrodynamic radius distribution of the PI/PS-b−P2VP hollow spheres in THF with differing composition. In the final solution, $C_{PS-b-P2VP} = 1.0 \times 10^{-4}$ g/mL; C_{PI} is shown in the legend. The inset is the SEM observation of hollow spheres with a PI/PS-b−P2VP weight ratio of 10:1.

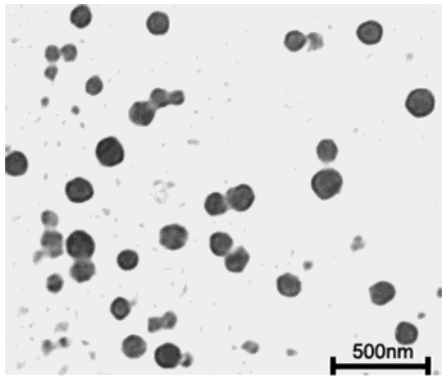

Figure 10. Morphologies of P2VP-block crosslinked hollow spheres of PAE/PS-b−P2VP (10:1, w:w) observed by TEM.

were very narrow as indicated by the low PDI values (0.01−0.09). The results clearly demonstrated that self-assembly of the block copolymers in the common solvent could be realized by grafting "rodlike" oligomers onto one block via hydrogen bonding.

The DLS data were summarized in Table 3. $\langle R_h \rangle$ of the aggregates with different compositions were around 60 nm and increased slightly with a decrease in the weight ratio of PAE/PS-b−P2VP from 10.0 to 5.0. It is worth noting that the nanoaggregates here are much smaller than the particles with the same weight ratio from PAE/P2VP. This means that the PS block promotes fine dispersion of the particles, this leads to much smaller nanoaggregates in THF. Considering the stabilization effect of the shell block in ordinary polymeric micelles,[24] it would be reasonable to assume that the PS block forms the outer shell. In other words, this approach enables one to adjust the dimensions of the supramolecular aggregates besides, as reported previously, changing the "graft" density.[19,20] Furthermore, the three-dimensional morphology of the particles was studied by SEM on silicon substrate. As shown in the inset of Figure 8, there are numerous folds on the nanoaggregates; this

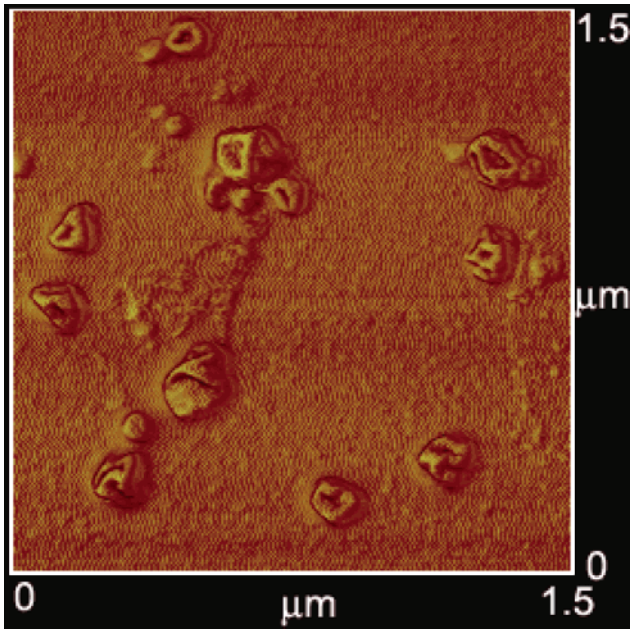

Figure 11. Phase-contrast AFM picture of P2VP block crosslinked hollow spheres of PAE/PS-b−P2VP(10:1, w:w).

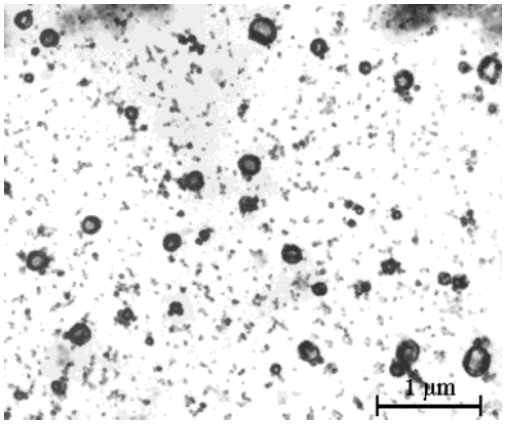

Figure 12. Morphologies of PAE crosslinked hollow spheres of PAE/PS-b−P2VP (10:1, w:w) observed by TEM.

is characteristic of polymeric hollow particles. [12a] The flattened appearance of the hollow particles should be formed under the high-vacuum condition for sample preparation. The particle size found by SEM is comparable with the DLS results. Based on the analysis above, the hollow particles should have a block copolymer outer shell and PAE inner shell.

We also found that the hollow particles could be obtained by assembly of PI and the block copolymer (Figure 9), but the micellar size was much larger than that of hollow particles of PS-b−P2VP and PAE. The morphology of the hollow particles from PI and PS-b−P2VP also was observed by SEM (inset in Figure 9). The images are quite similar to the case of PAE and the block copolymer.

Considering the fact that all of the components here, that is, PAE (PI), PS block, and P2VP block, are soluble in their common solvent and the interactions between the carboxyl ends of PAE (PI) and pyridene units would not substantially affect the solubilities of the polymer chains, it is clear that the micellization process is not caused by solubility difference. This rigid chain-assisted micellization of the block copolymers is associated with a new mechanism. The interaction between PAE (PI) and the pyridine units favors gathering of PAE surrounding P2VP, and the tendency of parallel packing of the grafted rigid chains promotes the assembly of the block copolymers forming the shell of the hollow spheres.

Structure Stabilization of Hollow Spheres of PAE and PS-b−P2VP. Based on the fact that P2VP block can be chemically crosslinked by using 1,4-dibromobutane,[25] and that PAE is easy to be photocrosslinked,[19] two approaches to stabilize the hollow particles of PAE/PS-b−P2VP are possible. For this propose, 100 mol % of 1,4-dibromobutane based on the pyridine units was added into the PAE/block copolymers with a total concentration of 1.1×10^{-3} g /mL, and the mixture was kept on 45 °C for 2 days. In a control experiment, the hollow-spheres solution without the crosslinker was treated at the same condition. In both cases, an equivolume DMF, which could cause dissociation of the interpolymer hydrogen bonding leading to decomplexation, was added to the solution after the reaction. For the control, the aggregates disappeared in DMF/THF. However, as shown in Table 3, after the reaction, the hollow particles kept a monomodal distribution, which implied that no interparticle reaction occurred. This meant that the structure of the hollow particles was successfully locked. This result strongly supports our proposal about the structure of the hollow particles, that is, the PS blocks existing in the outer shell that prevent the interparticle reactions. Armes et al.[26] have reported the role of the outer shell in preventing intermiceller crosslinking of the micelles of block copolymers at a high solid content. Our DLS measurements show that the crosslinked hollow spheres have a larger radius, of about 75 nm, compared with the 60 nm radius for the precursors. This size expansion should be a result of swelling of block copolymer shell after adding DMF. The broader distribution of the crosslinked hollow particles could

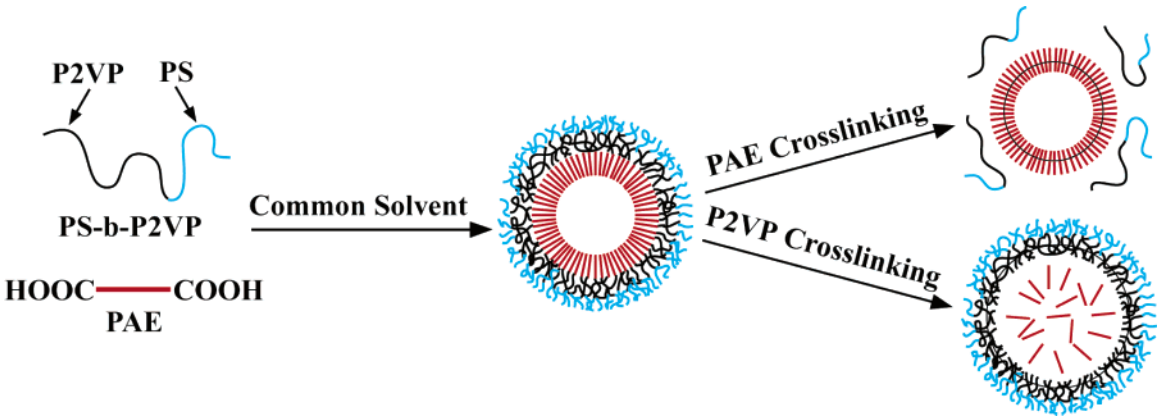

Figure 13. Schematic illustration of the formation of hollow spheres of block copolymer PS-b−P2VP and PAE and of the structure stabilization.

be caused by an inhomogeneous crosslinking reaction because no stirring was done during the reaction.

The morphology of the crosslinked particles in the dried state has been investigated by a transmission electronic microscope (TEM) on carbon-coated copper grids (Figure 10) and by an atomic force microscope (AFM) on silicon substrate (Figure 11). Figure 10 shows a clear structure of the shell crosslinked micelles. The outermost dark shell with the thickness of 15 nm was attributed to the PS-b−P2VP block copolymer. Although we can see a thin and dark outline of the particles, no bright domains within the particles can be found. This is obviously different from the hollow spheres produced from the NCCM of P4VP and hydroxyl-containing polystyrene, PS(OH).[18c] In the latter case, the cavitation of the crosslinked micelles was realized just by dissolution of the core of PS(OH). Considering the stiff structure of PAE, it is probably not as easy for coil PS(OH) oligomers to penetrate through the crosslinked outer shell. As a result, they could distribute homogeneously within the particles. The technique of AFM is useful for visualizing the three-dimensional shape of nanoaggregates. The flattened particles shown in Figure 11 could be a result of the collapse of the thin-layer hollow sphere on the substrate.

Cross-linking the PAE layer of the PAE/PS-b−P2VP aggregates was performed as described above by photocrosslinking. Again, the structure stabilization was confirmed by adding equivolume DMF to the THF solution. Meanwhile, it was found that the size of the crosslinked spheres in THF/DMF decreased. This was quite similar to what was reported in our previous study for crosslinked PAE/P4VP hollow spheres.[19] In THF/DMF, the hydrogen bonding between the PAE and block copolymer dissociates and then the outer shell disappears; this leads to a smaller-sized sphere. However, the size decrease of the spheres does not seem very significant (Table 3). Perhaps the size decrease caused by losing the block copolymers is partially compensated by the larger swelling of the PAE network in THF/DMF than in pure THF. The TEM images of the crosslinked PAE shells are shown in Figure 12. The central cavity is visualized by the obvious contrast between the central and outer part. Besides the hollow spheres, there is a large amount of irregular, small spots, which can be obviously attributed to the 'free' block copolymers produced in DMF/THF mixture as a result of dissociation of the hydrogen bonding between the end groups of PAE and P2VP blocks. Finally, we would like to emphasize that by crosslinking different parts of the hollow spheres of PAE/PS-b−P2VP, we are able to produce nanocages totally different in chemistry. By crosslinking PAE, we obtained polyimide-based hollow spheres with a central cavity. By crosslinking PS-b−P2VP, we obtained block-copolymer-based nanocages with PAE uniformly distributed inside. A schematic illustration of these processes is shown in Figure 13.

Acknowledgment. The work was financially supported by NNSFC (No. 50333010, No. 50173006).

References and Notes

(1) (a) Muthukumar, M.; Ober, C. K.; Thomas, E. L. *Science* **1997**, *277*, 1225. (b) Stupp, S. I.; LeBonheur, V.; Walker, K.; Li, L. S.; Huggins, K. E.; Keser, M.; Amstutz, A. *Science* **1997**, *276*, 384. (c) Klok, H. A.; Lecommandoux, S. *Adv. Mater.* **2001**, *13*, 1217. (d) Dennis, E. D.; Eisenberg, A. *Science* **2002**, *297*, 967. (e). Bergbreiter, D. E. *Angew. Chem., Int. Ed. Engl.* **1999**, *38*, 2870. (f) Caruso, F.; Caruso, R. A.; Möhwald, H. *Science* **1998**, *282*, 1111.

(2) Hadjichristidis, N.; Pispas, S.; Floudas, G. *Block Copolymers: Synthetic Strategies, Physical Properties, and Applications*; John Wiley & Sons: 2003.

(3) (a) Tu, Y.; Wan, X.; Zhang, D.; Zhou, Q.; Wu, C. *J. Am. Chem. Soc.* **2000**, *122*, 10201; (b) Svensson, M.; Alexandridis, P.; Linse, P. *Macromolecules* **1999**, *32*, 637; (c) Butun, V.; Armes, S. P.; Billingham, N. C. *Macromolecules* **2001**, *34*, 1148.

(4) (a) Liu, S. Y.; Billingham, N. C.; Armes, S. P. *Angew. Chem., Int. Ed.* **2001**, *40*, 2328; (b) Gohy, J.; Antoun, S.; Jérôme, R. *Macromolecules* **2001**, *34*, 7435.

(5) Wu, C.; Niu, A. Z.; Leung, L. M.; Lam, T. S. *J. Am Chem. Soc.* **1999**, *121*, 1954.

(6) (a) Harada, A.; Kataoka, K. *Macromolecules* **1995**, *28*, 5294; (b) Kabanov, A. V.; Bronich, T. K.; Kabanov, V. A.; Yu, K.; Eisenberg, A. *Macromolecules* **1996**, *29*, 6797.

(7) Liu, S. Y.; Zhu, H.; Zhao, H. Y.; Jiang, M.; Wu, C. *Langmuir* **2000**, *16*, 3712.

(8) (a) Kabanov, A. V.; Bronich, T. K.; Kabanov, V. A.; Yu, K.; Eisenberg, A. *J. Am. Chem. Soc.* **1998**, *120*, 9941. (b) Gohy, J. F.; Mores, S.; Varshney, S. K.; Jérôme, R. *Macromolecules* **2003**, *36*, 2579. (c) Eisenberg, A.; Szoka, Jr. F. C.; Kabanov, A. V. *J. Am. Chem. Soc.* **2002**, *124*, 11872.

(9) Peng, H.; Chen, D.; Jiang, M. *Langmuir* **2003**, *19*, 10989

(10) (a) Huang, H. Y.; Remsen, E. E.; Kowalewski, T.; Wooley, K. L. *J. Am. Chem. Soc.* **1999**, *121*, 3805. (b) Zhang, Q.; Remsen, E. E.; Kowalewski, T.; Wooley, K. L. *J. Am. Chem. Soc.* **2000**, *122*, 3642.

(11) (a) Stewart, S.; Liu, G. *J. Chem. Mater.* **1999**, *11*, 1048. (b) Ding, J. F.; Liu, G. J. *J. Phys. Chem. B* **1998**, *282*, 1111.

(12) (a) Donath, E.; Sukhorukov, G. B.; Caruso, F.; Davis, S. *Angew. Chem., Int. Ed. Engl.* **1998**, *37*, 2202; (b) Caruso, F.; Lichtenfeld, H.; Donath, E.; Möhwald, H. *Macromolecules* **1999**, *32*, 2317; (c) Caruso, F.; Möhwald, H. *J. Am. Chem. Soc.* **1999**, *121*, 6039; (d) Gao, C.; Donath, E.; Möhwald, H.; Shen, C. *Angew. Chem., Int. Ed.* **2002**, *41*, 3789.

(13) (a) Hotz, J.; Meier, W. *Langmuir* **1998**, *14*, 1031; (b) Meier, W. *Chimia* **1999**, *53*, 214; (c) Okubo, M.; Konishi, Y.; Minami, H. *Colloid Polym. Sci.* **1998**, *276*, 638; (d) Emmerich, O.; Hugenberg, N.; Schmidt, M.; Sheiko, S. S. *Adv. Mater.* **1999**, *11*, 1299; (e) Jang, J.; Ha, H. *Langmuir* **2002**, *18*, 5613; (f) Zha, L. S.; Zhang, Y.; Yang, W. L.; Fu, S. K. *Adv. Mater.* **2002**, *14*, 1090; (f) Kamata, K.; Lu, Y.; Xia, Y. *J. Am. Chem. Soc.* **2003**, *125*, 2384; (g) Beil, J. B.; Zimmerman, S. C. *Macromolecules* **2004**, *37*, 778. (h) Hotz, J.; Meier, W. *Adv. Mater.* **1998**, *10*, 1387.

(14) (a) Jenekhe, S. A.; Chen, X. L. *Science* **1998**, *279*, 1903. (b) Jenekhe, S. A.; Chen, X. L. *Science* **1999**, *283*, 372.

(15) Breiteukamp, K.; Emrick, T. *J. Am. Chem. Soc.* **2003**, *125*, 12070.

(16) Wong, S. M.; Cha, J. N.; Choi, K. S.; Deming, T. J.; Stucky, G. D. *Nano Letters* **2002**, *2*, 583;

(17) Jungmann, W.; Schmidt, M.; Ebenhoch, J.; Weis, J.; Maskos, M. *Angew. Chem., Int. Ed.* **2003**, *42*, 1714.

(18) (a) Yuan, X. F.; Jiang, M.; Zhao, H. Y.; Wang, M.; Wu, C. *Langmuir* **2001**, *17*, 6122. (b) Wang, M.; Zhang, G. Z.; Chen, D. Y.; Jiang, M.; Liu, S. Y. *Macromolecules* **2001**, *34*, 7172. (c) Wang, M.; Jiang, M.; Ning, F. L.; Chen, D. Y.; Liu, S. Y.; Duan, H. W. *Macromolecules* **2002**, *35*, 5980. (d) Liu, X. Y.; Jiang, M.; Yang, S. L.; Chen, M. Q.; Chen, D. Y.; Yang, C.; Wu, K. *Angew. Chem., Int. Ed.* **2002**, *41*, 2950. (e) Duan, H. W.; Chen, D. Y.; Jiang, M.; Gan, W. J.; Li, S. J.; Wang, M.; Gong, J. *J. Am. Chem. Soc.* **2001**, *123*, 12097.

(19) Kuang, M.; Duan, H. W.; Wang, J.; Chen, D. Y.; Jiang, M. *Chem. Commun.* **2003**, 496.

(20) Duan, H. W.; Kuang, M.; Wang, J.; Chen, D. Y.; Jiang, M. *J. Phys. Chem. B* **2004**, *108*, 550.

(21) Zhao, H. Y.; Douglas, E. O.; Harrison, B. S.; Schanze, K. S. *Langmuir* **2001**, *17*, 8428.

(22) Ma, Y. H.; Cao, T.; Webber, S. E. *Macromolecules* **1998**, *31*, 1773.

(23) Liu, S. Y.; Zhang, G. Z.; Jiang, M. *Polymer* **1999**, *40*, 5449.

(24) Webber, S. E. *J. Phys. Chem. B* **1998**, *102*, 2618.

(25) Chen, D. Y.; Peng, H. S.; Jiang, M. *Macromolecules* **2003**, *36*, 2576.

(26) Bütün, V.; Wang, X.-S.; de Paz Báñez, M. V.; Robinson, K. L.; Billingham, N. C.; Armes, S. P. *Macromolecules* **2000**, *33*, 1.